Proc. Indian Acad. Sci. (Chem. Sci.), Vol. 98, Nos 1 & 2, January 1987, pp. 99–114.

Structural and electronic properties of six-coordinate Lewis-base adducts of iron(III) Schiff-base complexes. Crystal structure and magnetism of the high-spin complex [(imidazole)Fe(salen)(NCS)]–0·5 MeOH and of a related complex containing two dissimilar axial ligands

BRENDAN J KENNEDY, KEITH S MURRAY *, PETER R ZWACK, ERNST HORN†, MICHAEL R SNOW† and EDWARD R T TIEKINK†

Department of Chemistry, Monash University, Clayton, Victoria 3168, Australia
† Department of Physical and Inorganic Chemistry, University of Adelaide, Adelaide, South Australia 5001, Australia

Abstract. The structural and electronic properties of two high-spin iron(III) Schiff-base complexes [(imd)Fe(salen)(NCS)] (I) and [(imd)Fe(salen)(N_3)] (II) are described. Crystals of I as a hemimethanol solvate, $(C_3H_4N_2)Fe(C_{16}H_{14}N_2O_2)(NCS).0{\cdot}5\ CH_3OH$, crystallize in the triclinic space group $P\bar{1}$ with unit cell dimensions a = 14·278(4), b = 16·932(4), c = 9·057(4) Å, α = 97·40(3), β = 92·07(3), γ = 85·32(2)° and Z = 4. The structure was refined by a block-matrix least-squares procedure to final R 0·050 and R_w 0·057 using 3127 unique reflections with $I > 2{\cdot}5\ \sigma(I)$. Complex I is one of the few structurally characterized examples of six-coordinate Lewis-base adducts in which there are two different axial ligands. The in-plane Fe–N distances, 2·12 Å (av) are characteristic of S = 5/2 Fe^{III}. The Fe–N (imidazole) distance of 2·149(5) Å is similar to that in related high-spin imidazole-Fe^{III} complexes. Non-linear Fe–NCS bonding is observed (Fe–N–C = 159·0(5)°) as in related six-coordinate Fe^{III} porphyrin and methemoglobin isothiocyanate species. Mössbauer spectra of I and II between 295 and 4·2 K are symptomatic of S = 5/2 Fe^{III}. The nature of the asymmetry of the quadrupole doublet as a function of temperature points to zero field splitting of the $^6A_1$ ground state having a negative value of the axial ZFS parameter, D. These are new additions to the few known examples of negative D in Fe^{III}-tetradentate chelating systems, and contrast for instance with aquo-imidazole Fe^{III} salen adducts which we have recently shown to have positive D values. Spin-hamiltonian analyses of the 300–4·2 K χ_{Fe}/T data, assuming rhombic ligand field symmetry, yielded the following parameter sets; I: g = 1·98 ± 0·02, D = −2·4 ± 0·2 cm^{-1}, E = 0·6 ± 0·2 cm^{-1}. II: g = 2·00 ± 0·01, D = −1·4 ± 0·2 cm^{-1}, E = 0·4 ± 0·2 cm^{-1}. In the 77 K X-band ESR spectra of neat powdered samples of II: a line at g = 4·4 confirms the rhombic splitting, while the related spectrum for I shows a broad line at $g \sim 2{\cdot}1$. This somewhat unusual line position probably arises through solid state exchange effects since a g 4·3 signal is observed for a frozen glass spectrum.

Keywords. Six-coordinate Lewis-base adducts; iron(III) Schiff-base complexes; (imidazole)Fe(salen)(NCS); high spin complex; magnetism; Mossbauer spectra.

1. Introduction

Six-coordinate iron(III) complexes display a variety of electronic ground states, viz high-spin (S = 5/2), intermediate-spin (S = 3/2) or low-spin (S = 1/2) as well as spin-crossover behaviour (Mitra 1982). The precise nature of the ground state, which is often perturbed by other low lying states, is dependent on the bonding

* To whom all correspondence should be addressed.

properties of the coordinated ligands. Often small changes in the coordinating groups, and/or in the nature of non-coordinating anions or molecules of solvation can cause dramatic differences in the observed magnetic properties. These features are observed in complexes of type [Fe(tetradentate)L_2]X formed by the reaction of a Lewis-base (L) such as imidazole (imd) or pyridine (py) with tetradentate porphyrin or Schiff-base iron(III) complexes (Collman *et al* 1978; Nishida *et al* 1975, 1977; Scheidt *et al* 1979, 1983a; Hill *et al* 1979; Scheidt and Reed 1981; Gregson 1981; Maeda *et al* 1982; Ohshio *et al* 1983; Kennedy 1984; Kennedy *et al* 1987).

Addition of a Lewis-base to these complexes is thought to proceed in two stages (La Mar and Walker 1972; Walker *et al* 1976; Satterlee *et al* 1976)

$$[Fe^{III}(\text{tetradentate})L]^+ + L \overset{K_1}{\rightleftharpoons} [Fe^{III}(\text{tetradentate})L]^+$$

$$[Fe^{III}(\text{tetradentate})]^+ + L \overset{K_2}{\rightleftharpoons} [Fe^{III}(\text{tetradentate})L_2]^+$$

Formation and isolation of the *bis*-adduct is usually favoured in comparison to the mono-adduct and consequently many studies of the structural and magnetic properties of the *bis* adducts have been made. However, from the bioinorganic point of view, since many heme proteins contain only one bonded axial histidine residue, considerable interest has evolved recently in the synthesis and study of mono-imidazole adducts of these Fe^{III} chelates. Unfortunately the isolation of pure crystalline samples of such adducts has often proved difficult and this has therefore impeded progress in obtaining mono-base model compounds.

Recently, however, Scheidt and co-workers have reported structural studies on some porphyrin complexes of the type [Fe(por)(py)X] (X = NCS^-, N_3^-, CN^-; por = TPP^{2-}, OEP^{2-}) (Scheidt *et al* 1982, 1983b; Adams *et al* 1979). Variations in the porphyrin and X ligands led to high-spin or high-spin $\rightleftharpoons$ low-spin crossover complexes being obtained. A recently isolated phase of [Fe(TPP)(py)(NCS)] contains both of these electronic forms (Geiger *et al* 1985). However, the presence of variable amounts of apparently solvated Lewis base molecules has made a rigorous study of the magnetic properties of these six-coordinate moieties difficult. Our own recent work on the related Schiff-base systems (Kennedy 1984; Kennedy *et al* 1984, 1985, 1987) has indicated that, with suitable care, the mixed ligand complexes could be isolated, without containing any extra Lewis-base molecules. In this paper we describe the crystal structure of one such compound, [(imd)-Fe(salen)(NCS)], I, and relate the structural features to the electronic properties of the molecule. A detailed investigation of magnetic susceptibilities, ESR and Mössbauer spectra for this d^5 high-spin complex has yielded information on zero-field splitting of the $^6A_1$ ground state. Similar data are discussed for the analogous azido complex, [(imd)Fe(salen)(N_3)] (II). The crystal structure is not available for II but that of the related cobalt(III) complex [(py)Co(acen)(N_3)] is known (Clearfield *et al* 1978).

2. Experimental section

2.1 *Synthesis*

[*Fe*(*salen*)(*NCS*)] and [Fe(salen)(N_3)] were prepared as described by Gullotti *et al* (1977).

[(*imd*)Fe(salen)(NCS)] (I): 0·5 g of [Fe(salen)(NCS)] were suspended in 40 ml of absolute methanol and 0·5 g of imidazole added. The solution was then refluxed for 15 minutes during which time most of the solid dissolved. Any undissolved solid was then removed from the hot solution and, on cooling overnight, small black crystals were deposited. These were filtered, washed twice with ice-cold methanol, and then dried in air.

The same crystalline product could be obtained by refluxing Fe(salen)Cl and excess imidazole in methanol for 10 minutes, followed by addition of a 2 molar excess of sodium thiocyanate. IR spectrum: ν(NCS) 2080 cm^{-1}.

[(*imd*)*Fe*(*salen*)(N_3)] (II): This compound was prepared from [Fe(salen)(N_3)] in an analogous manner to that described above. IR spectrum: $\nu(N_3)$ 2080 cm^{-1}.

Satisfactory analytical data were obtained for both complexes.

Crystals of [(imd)Fe(salen)(NCS)] suitable for the x-ray diffraction study were obtained by slow evaporation of a methanol solution. The crystal structure showed the presence of 0·5 mol of methanol of solvation.

2.2 *Physical methods*

Magnetic susceptibilities were measured in a field of 10 kG on an Oxford Instruments Faraday Balance (Mackey *et al* 1976). Samples were carefully checked for any anomalous field dependence at both 4·2 K and 300 K, but none was found to be present.

ESR and Mössbauer spectra were obtained as described elsewhere (Mitchell *et al* 1977). The isomer shifts are relative to iron metal at room temperature.

2.3 *X-ray crystal structure determination of* I

A black-prism was mounted on a glass fibre and coated with cyano-acrylate super glue. Lattice parameters at 295 K were determined by a least-squares procedure on the setting angles of 25 reflections measured with MoK_α radiation (λ 0·71073 Å) on an Enraf-Nonius CAD4 diffractometer. Intensity data on this crystal were collected using an ω: $(n/3)\theta$ scan where $n(= 2)$ was optimized by profile analysis of a number of representative reflections. No significant decomposition of the crystal occurred during the data collection. Correction was applied for Lorentz and polarization effects using the program SUSCAD (Guss 1979) and for absorption using the appropriate procedure in SHELX (Sheldrick 1976). Crystallographic data are summarized in table 1.

The structure was solved using the program MULTAN and refined by a block-matrix least-squares procedure in which the function $\Sigma\omega\Delta^2$ was minimized (Guss 1979). Anisotropic thermal parameters were introduced for all non-hydrogen atoms and a weighting scheme, $1{\cdot}47/[\sigma^2(F) + 0{\cdot}0021|F|^2]$, included. The refinement converged with final values for R and R_w 0·050 and 0·057, respectively. Hydrogen atoms were not included in the model and no correction was made for extinction. The analysis of variance showed no special features and the maximum residual electron density peak in the final difference map was 0·52 $eÅ^{-3}$. The assignment of the 'ambiguous' N(5) and C(19) atoms of the imidazole group was confirmed by interchanging the atoms and refining the model. The result of the procedure was an increase in R and the presence of non-sensible thermal ellipsoids

Table 1. Summary of the crystallographic data for (imd)Fe(salen)(NCS)·0·5 MeOH (I).

Formula	$C_{20.5}H_{16}N_5O_{2.5}SFe$
mol. wt.	460·3
crystal system	triclinic
space group	$P\bar{1}$ (C_i^1, No. 2)
a, Å	14·278(4)
b, Å	16·932(4)
c, Å	9·057(4)
α, °	97·40(3)
β, °	92·07(3)
γ, °	85·32(2)
U, Å^3	2163·4
d_{calcd} (d^a_{obs}), Mg/m^3	1·41 (1·45)
crystal dimensions, mm^3	0·15 × 0·45 × 0·50
radiation	MoK_α (graphite monochromator)
absorption coefficient, μ, mm^{-1}	0·785
transmission factors (max/min)	0·886, 0·734
temperature K	297
omega scan angle, °	(1·90 + 0·35 tan θ)
horizontal counter apertures, mm	(2·40 + 0·5 tan θ) ·
data collected	$1{\cdot}3 \leq \theta \leq 21°$, (± h, ± k, l)
total reflections	4581
R^b_{merge}	0·023
unique data, $I \geq 2{\cdot}5\sigma(I)$	4376, 3126
R (R_w)	0·050 (0·057)
largest Δ/σ, eÅ^{-3}	0·52

Scattering factors for neutral Fe were from Ibers and Hamilton (1974), the terms having been corrected for $\Delta f'$ and $\Delta f''$ and those of the remaining atoms were those incorporated in the SHELX system. Final fractional coordinates are listed in table 2. The associated anisotropic thermal parameters are given in the Supplementary Material as are lists of observed and calculated structure factors and complete lists of bond lengths and bond angles.

3. Results and discussion

The products from the reaction of Fe(salen)X (X = SCN, N_3) with excess imidazole are the mixed ligand complexes [(imd)Fe(salen)(NCS)] (I) and [(imd)Fe(salen)-(N_3)] (II). Even when extremely large excesses of the Lewis base were used there is no evidence to suggest that any *bis*-adducts are present in the polycrystalline products although, as shown below, such species can form in solution and are expected to be present in the reaction mixture (Kennedy *et al* 1985, 1987). The relative stability of the mixed ligand complex in the present case can be compared to the complicated equilibria found for the related iron(III) porphyrin complexes where the formation of the mono-imidazole adducts is favoured only for a very small ratio of imidazole to porphyrin with larger ratios yielding the corresponding *bis*-adduct (Scheidt *et al* 1982, 1983; Adams *et al* 1979).

Repeated attempts to isolate the *bis* adducts $[Fe(salen)(imd)_2]X$ (X = SCN or N_3) were unsuccessful as were attempts to prepare the analogous chloride complex $[Fe(salen)(imd)_n]Cl$ (n = 1 or 2). Indeed with the chloride only the starting product or the μ-oxo dimer $[Fe(salen)]_2O$ could be isolated from the reaction solutions. The *bis*-imidazole compounds can be crystallized when a large anion such as ClO_4^-, BF_4^- or PF_6^- is present. The structures and properties of these compounds are described elsewhere (Kennedy 1984; Kennedy *et al* 1987).

3.1 *Crystal and molecular structure of* I

The numbering scheme is shown in figure 1, which highlights the molecular structure of the complex. There are two crystallographically distinct molecules in the asymmetric unit; the numbering of the second molecule is the same as in figure 1 but with an asterisk on each atom. Individual bond lengths and angles in the two molecules are very similar with only minor differences noted (tables 3 and 4). The different molecules are seen in the crystal packing diagram shown in figure 2. Also

Table 2. Non hydrogen atom coordinates for (imd)Fe(salen)(NCS) – 0·5 MeOH(I)[a,b].

Atom	x	y	z	Atom	x	y	z
Fe	55673(6)	76766(5)	2628(9)	C(13)	4870(5)	6000(4)	3878(8)
Fe(')	03895(6)	72012(5)	31889(9)	C(14)	4303(5)	6284(5)	5062(9)
S(1)	3016(1)	6060(1)	−1264(2)	C(15)	3977(5)	7104(5)	5270(8)
S(1')	7627(1)	5890(1)	4045(2)	C(16)	4227(5)	7626(4)	4299(7)
O(1)	5278(3)	8633(2)	−667(4)	C(17)	4822(4)	7323(4)	3082(7)
O(2)	5058(3)	7854(2)	2205(4)	C(18)	7427(5)	7817(4)	2124(7)
O(1')	9756(3)	8066(3)	4459(4)	C(19)	7987(5)	8966(5)	1849(10)
O(2')	9859(3)	7319(2)	1283(4)	C(20)	7199(5)	8867(5)	945(9)
N(1)	4323(4)	7189(3)	−530(6)	C(1")	8643(4)	6205(3)	3764(6)
N(2)	6166(3)	7152(3)	−1782(5)	C(2")	9911(5)	8325(4)	5905(7)
N(3)	6082(3)	6528(3)	716(6)	C(3")	9360(7)	8993(6)	6510(9)
N(4)	6862(3)	8141(3)	1126(5)	C(4")	9473(8)	9287(6)	8023(11)
N(5)	8118(4)	8313(3)	2606(6)	C(5")	10107(8)	8911(6)	8923(10)
N(1')	9358(4)	6433(3)	3559(6)	C(6")	10657(6)	8234(5)	8342(8)
N(2')	11137(3)	6829(3)	5040(5)	C(7")	10540(5)	7940(4)	6829(7)
N(3')	11252(3)	6231(3)	2213(6)	C(8")	11120(5)	7197(4)	6365(7)
N(4')	11468(3)	7966(3)	2851(6)	C(9")	11644(5)	6030(4)	4791(8)
N(5')	12531(4)	8521(4)	1686(7)	C(10")	12017(5)	5927(5)	3183(8)
C(1)	3788(4)	6718(4)	−829(7)	C(11")	11110(5)	5841(4)	892(7)
C(2)	5599(4)	8876(4)	−1898(7)	C(12")	10386(5)	6093(4)	−156(7)
C(3)	5378(5)	9677(4)	−2113(7)	C(13")	10328(6)	5583(5)	−1525(9)
C(4)	5682(6)	9954(5)	−3407(9)	C(14")	9659(7)	5766(5)	−2599(8)
C(5)	6193(6)	9449(6)	−4459(9)	C(15")	9051(5)	6449(5)	−2344(8)
C(6)	6396(6)	8671(6)	−4252(8)	C(16")	9093(5)	6977(5)	−1038(8)
C(7)	6101(4)	8354(4)	−2964(7)	C(17")	9789(4)	6792(4)	82(7)
C(8)	6314(5)	7509(4)	−2910(7)	C(18")	12066(5)	7853(5)	1759(8)
C(9)	6346(6)	6274(4)	−1913(9)	C(19")	12209(6)	9064(5)	2818(12)
C(10)	6728(5)	6074(4)	−387(8)	C(20")	11559(6)	8732(5)	3521(11)
C(11)	5771(4)	6147(4)	1733(8)	O	6598(4)	889(3)	560(7)
C(12)	5136(4)	6521(4)	2877(7)	C	6967(7)	1096(7)	2031(13)

[a] Fe coordinates $\times 10^5$; other atom coordinates $\times 10^4$

[b] Atoms labelled with an asterisk refer to the second distinct molecule in the asymmetric unit. Atom C and O are for methanol.

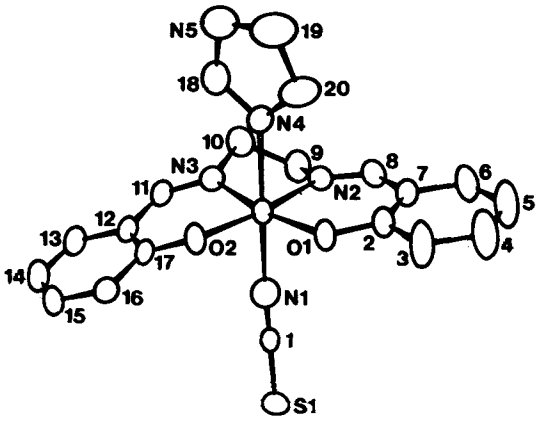

Figure 1. Molecular structure and numbering scheme for I. Atoms otherwise not indicated are carbon atoms.

evident are methanol molecules of solvation which are present in the ratio of one MeOH to two [(imd)Fe(salen)(NCS)]. Both of the molecules of I are involved in weak intermolecular hydrogen-bonding to the solvate molecule. The two closest intermolecular contacts in the structure occur between the oxygen atom of MeOH and $O(1)^a$ of 2·736 Å and $N(5')^b$ of 2·755 Å (where superscripts *a* and *b* refer to the symmetry operations $1-x, 1-y, -z$, and $2-x, 1-y, -z$, respectively). In this context it is noteworthy that the Fe–O(1) distance in each of the two molecules is not significantly different from the Fe–O(2) distance so that it is unlikely that the presence of the intermolecular contact described above influences the nature of the Fe atom environment.

Figure 1 shows that iron exists in a distorted octahedral environment defined by the O(1), O(2), N(3), N(2) donor atoms of salen in the basal plane, the N(1) atom of the end-on isothiocyanato ligand, and the N(4) atom of imidazole. Distortions from the ideal octahedral angles arise, in part, as a result of the conformation of the salen ligand and are similar to those found in related systems (Calligaris *et al* 1972). The central ethylenediamine FeN_2C_2 ring adopts the 'gauche' (meso) conformation while the two halves of the salen ligand are essentially coplanar. The Fe-salen geometry is very similar to that recently observed in the high-spin complex $[Fe(salen)(imd)_2]PF_6$ for which we have noted a possible relationship between conformation and spin-state (Kennedy *et al* 1987). Some pertinent comparisons with this PF_6^- salt (the latter in parentheses) are: angles O(2)–Fe–O(1) = 107·9(2)° (107·2(2)°), O(1)–Fe–N(2) = 87·1(2)° (88·2(2)°), N(2)–Fe–N(3) = 76·8(2)° (76·8(2)°); distances N(2) . . . N(3) = 2·628(8) Å (2·652(9) Å), O(1) . . . O(2) = 3·101(7) Å (3·064(7) Å). The iron atom in complex I sits in the plane of the salen donor atoms; the mean planes and displacements therefrom are given in table 5.

It has been noted in related studies (Kennedy *et al* 1985, 1987; Calligaris *et al* 1972) that the length of the metal-imine bond is sensitive to the spin state of the metal ion. The metal ion in high-spin complexes form longer M–N bonds than in corresponding low-spin complexes. The Fe^{III}–N(imine) distances in high-spin complexes are normally in the range 2·05–2·15 Å, and in low-spin complexes in the range 1·90–1·96 Å. The Fe–N(2) and Fe–N(3) distances found for I are in the range

Table 3. Selected bond lengths (Å) in I. (Atoms marked with an asterisk refer to the second crystallographically distinct molecule in the asymmetric unit.)

O(1)–Fe	1·928(4)	O(1′)–Fe′	1·926(4)
O(2)–Fe	1·907(4)	O(2′)–Fe′	1·888(4)
N(2)–Fe	2·125(5)	N(2′)–Fe′	2·093(5)
N(3)–Fe	2·108(5)	N(3′)–Fe′	2·091(5)
N(1)–Fe	2·085(5)	N(1′)–Fe′	2·106(6)
N(4)–Fe	2·149(5)	N(4′)–Fe′	2·145(5)
C(2)–O(1)	1·345(8)	C(2′)–O(1′)	1·343(7)
C(17)–O(2)	1·344(8)	C(17′)–O(2′)	1·322(7)
C(7)–C(8)	1·445(10)	C(7′)–C(8′)	1·471(9)
C(12)–C(11)	1·450(9)	C(12′)–C(11′)	1·454(9)
C(8)–N(2)	1·284(9)	C(8′)–N(2′)	1·280(8)
C(11)–N(3)	1·299(9)	C(11′)–N(3′)	1·308(8)
N(2)–C(9)	1·478(9)	N(2′)–C(9′)	1·476(8)
N(3)–C(10)	1·481(8)	N(3′)–C(10′)	1·478(9)
C(9)–C(10)	1·536(11)	C(9′)–C(10′)	1·553(11)
N(1)–C(1)	1·149(8)	N(1′)–C(1′)	1·150(8)
C(1)–S(1)	1·633(6)	C(1′)–S(1′)	1·625(6)
C(18)–N(4)	1·331(8)	C(18′)–N(4′)	1·315(9)
C(18)–N(5)	1·371(9)	C(18′)–N(5′)	1·367(10)
C(19)–N(5)	1·370(10)	C(19′)–N(5′)	1·353(11)
C(19)–C(20)	1·375(11)	C(19′)–C(20′)	1·343(14)
C(20)–N(4)	1·388(10)	C(20′)–N(4′)	1·374(9)
C–O	1·426(13)		

Table 4. Selected bond angles (in degrees) for I. (Atoms marked with an asterisk refer to the second crystallographically distinct molecule in the asymmetric unit.)

O(2)–Fe–O(1)	107·9(2)	O(2′)–Fe′–O(1′)	103·4(2)
O(2)–Fe–N(3)	88·2(2)	O(2′)–Fe′–N(3′)	88·6(2)
N(3)–Fe–N(2)	76·8(2)	N(3′)–Fe′–N(2′)	78·1(2)
N(2)–Fe–O(1)	87·2(2)	N(2′)–Fe′–O(1′)	90·0(2)
N(2)–Fe–O(2)	164·4(2)	N(2′)–Fe′–O(2′)	166·6(2)
N(3)–Fe–O(1)	163·9(2)	N(3′)–Fe′–O(1′)	167·9(2)
N(4)–Fe–N(1)	177·8(2)	N(4′)–Fe′–N(1′)	178·4(2)
N(2)–C(8)–C(7)	124·2(6)	N(2′)–C(8′)–C(7′)	124·7(6)
N(3)–C(11)–C(12)	123·1(6)	N(3′)–C(11′)–C(12′)	123·4(6)
C(2)–C(7)–C(8)	125·3(6)	C(2′)–C(7′)–C(8′)	124·8(6)
C(11)–C(12)–C(17)	125·4(6)	C(11′)–C(12′)–C(17′)	124·9(5)
C(7)–C(2)–O(1)	122·2(6)	C(7′)–C(2′)–O(1′)	124·0(6)
C(12)–C(17)–O(2)	123·6(5)	C(12′)–C(17′)–O(2′)	122·6(5)
C(2)–O(1)–Fe	132·1(3)	C(2′)–O(1′)–Fe′	130·1(4)
C(17)–O(2)–Fe	129·5(3)	C(17′)–O(2′)–Fe′	130·6(4)
C(8)–N(2)–C(9)	118·7(5)	C(8′)–N(2′)–C(9′)	118·3(5)
C(11)–N(3)–C(10)	117·6(5)	C(11′)–N(3′)–C(10′)	118·9(5)
N(2)–C(9)–C(10)	106·8(5)	N(2′)–C(9′)–C(10′)	106·8(6)
N(3)–C(10)–C(9)	105·6(5)	N(3′)–C(10′)–C(9′)	107·3(5)
Fe–N(4)–C(18)	124·4(4)	Fe′–N(4′)–C(18′)	126·0(4)
Fe–N(4)–C(20)	127·9(4)	Fe′–N(4′)–C(20′)	127·4(5)
Fe–N(1)–C(1)	159·0(5)	Fe′–N(1′)–C(1′)	161·2(5)
N(1)–C(1)–S(1)	179·2(6)	N(1′)–C(1′)–S(1′)	179·4(6)

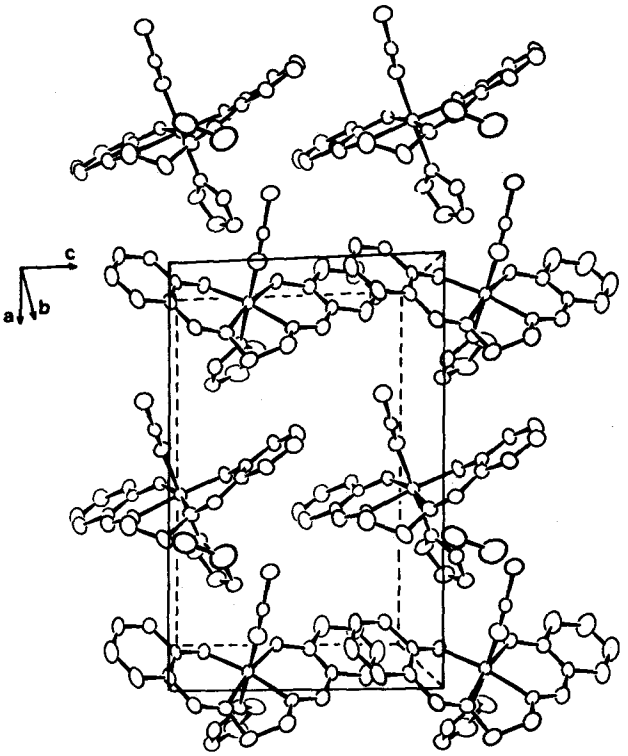

Figure 2. Crystal packing diagram for complex I.

Table 5. Mean planes in the two different molecules of (imd)Fe(salen)(NCS) of the asymmetric unit. Displacements in Å units.

Molecule 1		
	Mean plane equation	$-0{\cdot}041X-0{\cdot}033Y+0{\cdot}0007Z+1=0$
	"in-plane" atoms	Fe, 0; O(1), 0·025; O(2), −0·025; N(2), −0·028; N(3), 0·03
	"out-of-plane" atoms	C(9), −0·346; C(10), 0·3
Molecule 2		
	Mean plane equation	$-0{\cdot}074X-0{\cdot}036Y-0{\cdot}029Z+1=0$
	"in-plane" atoms	Fe′, 0·016; O(1′), 0·036; O(2′), −0·048; N(2′), −0·052; N(3′), 0·046
	"out-of-plane" atoms	C(9′), −0·416; C(10′), 0·31

2·09–2·15 Å which is indicative of a high-spin ground state for Fe^{III} in the complex and consistent with the spectroscopic and magnetic data (see below). This compares with corresponding Fe–N distances of 1·90–1·92 Å in the low-spin (low temperature) form of $[(imd)_2Fe(salen)](ClO_4)$ (Kennedy 1984; Kennedy *et al* 1987).

The Fe–N(imidazole) distance of 2·149(5) Å is very similar to that observed in high-spin *bis*-imidazole Fe^{III} salen systems (Kennedy *et al* 1987) and in high-spin $[(5Ph\text{-}imd)Fe(3MeO\text{-}salen)(H_2O)]BPh_4$ (Kennedy *et al* 1985). The geometric

features of the iron-isothiocyanate group are compared in table 6 with those for related Fe^{III} porphyrin complexes (Scheidt *et al* 1982; Geiger *et al* 1985). N–C and C–S distances are similar in all cases. The Fe–N distance for the lower-spin TPP complexes are notably shorter than for the two high-spin complexes. While the NCS moiety is linear as expected, the FeNC angle in I and in two forms of the TPP complex is somewhat bent. In the latter cases the non-linearity has been ascribed to packing interactions in the solid state. The same situation may apply in I although there do not appear to be any unusual intermolecular interactions other than those involving methanol and the salen group as described above. The related azido complex (Clearfield *et al* 1978), [(py)Co(acen)(N_3)], shows an even more acute Co–N–N angle of 116·9°, rather similar in magnitude to the Fe–N–C angle found in the ligand binding pocket of (NCS)-methemoglobin (120 ± 10°) (Korszun and Moffatt 1981).

3.2 *Mössbauer effect, ESR spectra and magnetism*

The zero-field Mössbauer spectrum of I measured between 4·2 and 300 K consists of a single asymmetrical doublet (figure 3). The values of the isomer shift and quadrupole splitting, obtained by fitting the spectra to two unconstrained Lorentzian lines are typical of high-spin iron(III) complexes (table 7) and are similar to the values observed in other six-coordinate high-spin Lewis base adducts of Fe(III)salen such as [Fe(3MeO-salen)(Ph-imd)(H_2O)]BPh_4 and [Fe(salen)$(imd)_2$]PF_6 (Kennedy *et al* 1985, 1987). At all temperatures the two lines have a difference in area of ≈ 10% which increases only slightly on cooling and is

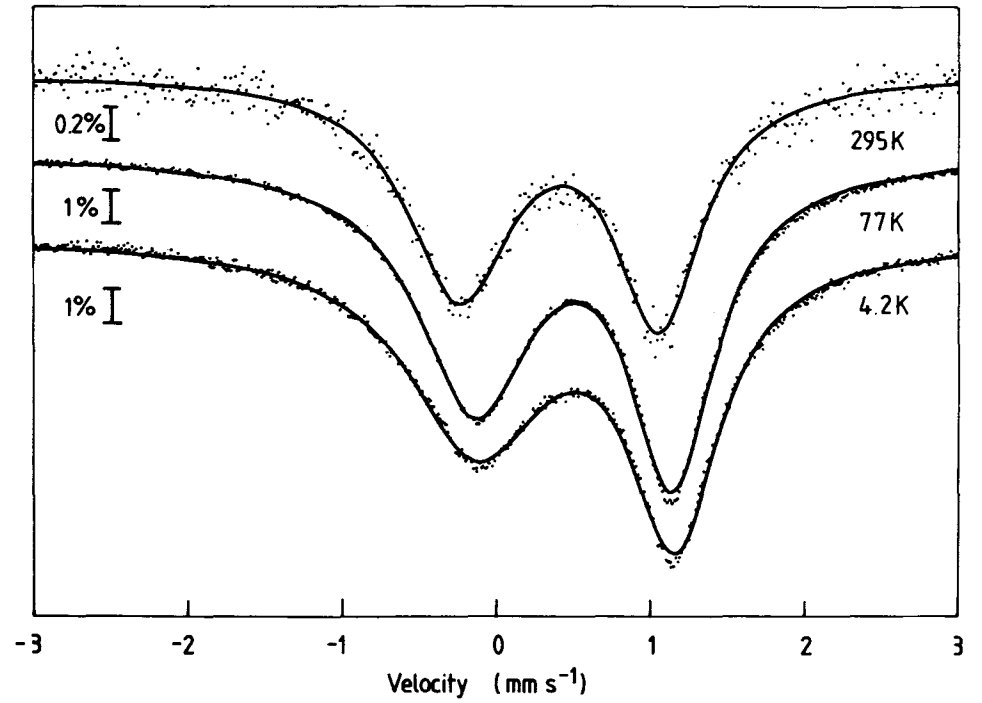

Figure 3. Mössbauer spectra of complex I in zero applied field at 295, 77 and 4·2 K.

Table 6. Fe–NCS geometry in [(imd)Fe(salen)(NCS)]0·5 MeOH I, and related porphyrin complexes at 295 K.

	I	[(py)Fe(OEP)(NCS)]	[(py)Fe(TPP)(NCS)]0·5 py	[(py)Fe(TPP)(NCS)]	
				Site 1	Site 2
Spin state	5/2	5/2	"1/2"	$1/2 \rightleftharpoons 5/2$	5/2
Fe–N (Å)	2·085	2·031	1·942	1·91	1·97
N–C (Å)	1·149	1·153	1·144	–	–
C–S (Å)	1·633	1·626	1·606	–	–
NCS (°)	179·2	179·6	177·0	–	–
FeNC (°)	159·0	176·0	155·6	175	139
reference	this work	(Scheidt *et al* 1982)	(Scheidt *et al* 1982)	(Geiger *et al* 1985)	(Geiger *et al* 1985)

Table 7. Zero field Mössbauer parameters.

Complex	T(K)	δ^a (mms^{-1})	ΔE_Q (mms^{-1})	half-width^b Γ_1, Γ_2	area ratio line 2/line 1	$I_2/I_1{}^c$
I	295	0·41	1·29	0·41, 0·33	0·90	1·1
	77	0·50	1·29	0·45, 0·33	0·93	1·28
	4·2	0·51	1·29	0·55, 0·35	0·91	1·40
II (fit 1)	295	0·38	0·92	0·56, 0·56	d	1·0
	77	0·52	0·93	0·59, 0·47	d	1·1
	4·2	0·48	0·98	0·49, 0·48	d	1·57
II (fit 2)	295	0·38	0·92	0·56, 0·56	d	1·0
	77	0·50	0·91	0·48, 0·51	d	1·29
		0·36^e	2·67	0·37, 0·37		
	4·2	0·49	0·89	0·40, 0·41	d	1·55
		0·36^e	2·67	0·38, 0·38		

^{a} relative to Fe. ^{b} half-width at half-height in mm s^{-1} for line 1 of the doublet at lower velocity and line 2 at higher velocity. ^{c} ratio of intensities. ^{d} area ratio not meaningful because of contribution of Gaussian base line curve (see text). ^{e} second weak doublet constrained to these values.

thought to arise from the Goldanskii-Karyagin effect (Karyagin 1963; Goldanskii *et al* 1968). The increase in the isomer shift at low temperatures is probably due to the second-order Doppler shift.

The increase in asymmetry of the peak intensities at lower temperatures can be explained in terms of spin–spin relaxation effects in a system where the $M_s = \pm 5/2$ Kramers doublet lies lowest (i.e. D, the axial ZFS parameter, is negative, Buckley 1971). When the $|\pm 5/2\rangle$ states lie lowest a quadrupole doublet will be observed if the rate of spin–spin relaxation, τ, is slower than ω_i^{-1} (where ω_i is the angular nuclear harmonic precession frequency). The spin–spin relaxation rate is expected to be slower at 4·2 K than at higher temperatures, since for spin flips induced by dipolar coupling between molecules, transitions between the $|+5/2\rangle$ and $|-5/2\rangle$ states are forbidden. The slowly relaxing $|\pm 5/2\rangle$ ground state results in preferential broadening of one line of the quadrupole doublet. At higher temperatures where the $|\pm 3/2\rangle$ and $|\pm 1/2\rangle$ doublets are also populated the asymmetry in peak height is expected to reach a minimum. If τ was greater than ω_i^{-1}, or even comparable with it at 4·2 K then magnetic hyperfine would be expected.

The Mössbauer spectra for the azide complex II at various temperatures are shown in figure 4. The spectra were less straightforward to fit than those for I since they are not fully relaxed and therefore a broad Gaussian baseline component was included in the fit. Also there is a weak low velocity shoulder present in the 4·2 K and 77 K spectra arising, possibly, from trace quantities of a low-spin species. The parameters for two separate fits are given in table 7. In both cases the isomer shifts and quadrupole splittings due to II are very similar. The δ values are similar to those in I while the ΔE_Q values are lower, probably because of a more symmetrical arrangement of the N_4O_2 donor set in the azido-complex. Fit 1 used two unconstrained Lorentzian lines together with a Gaussian base curve contributing about 50% of the area. While this fit reproduced the majority of the line-shape quite well it did not, of course, fit the shoulder at low velocity. The increase in

intensity asymmetry as the temperature decreased followed the same pattern as in I. In fit 2 a second doublet was included with parameters constrained to the values observed for low-spin *bis*-imidazole Fe^{III}-salen species (Kennedy *et al* 1987). This improved the overall fit of the lineshapes. Again, a broad Gaussian baseline curve was incorporated and contributed 33% (at 77 K) to 41% (at 4·2 K) of the area. The second (low-spin) doublet contributed only about 5% of the total area.

Despite the complexities of the line-fitting the temperature dependence of the Mössbauer spectra of II can be explained in a similar manner to that given for I and it appears that D is also negative in this complex. The sign of D found in the present compounds is the opposite to that observed in most other well characterized six-coordinate Fe^{III} Schiff-base complexes such as $[Fe(salen)(imd)_2]PF_6$ ($D = 0{\cdot}6\ cm^{-1}$), $[Fe(3MeO\text{-}salen)(5\text{-}Ph\text{-}imd)(H_2O)]BPh_4$ ($D = 5{\cdot}0\ cm^{-1}$) and the parent dimer $[Fe(salen)Cl]_2$ (Buckley *et al* 1970). However, some five-coordinate *bis*-bidentate Schiff-base complexes such as $[Fe(sal\text{-}N\text{-}ptolyl)_2Cl]$ also appear to have the $|\pm 5/2\rangle$ state lowest (Buckley 1971). The exact nature and magnitude of the ground state splitting in these types of compounds is apparently critically dependent on the number *and* nature of the coordinated ligands. This is well demonstrated in the seven-coordinate complexes $[Fe(N_5)X_2]$, ($X = SCN^-, N_3^-$; N_5 is a pentadentate macrocycle) where the sign of D changes from positive for $X = SCN^-$ to negative for $X = N_3^-$ (Scoville and Reiff 1983).

The temperature dependence of the magnetic moment for [(imd)Fe-(salen)(NCS)] is shown in figure 5 and is characteristic of a high-spin Fe^{III} system

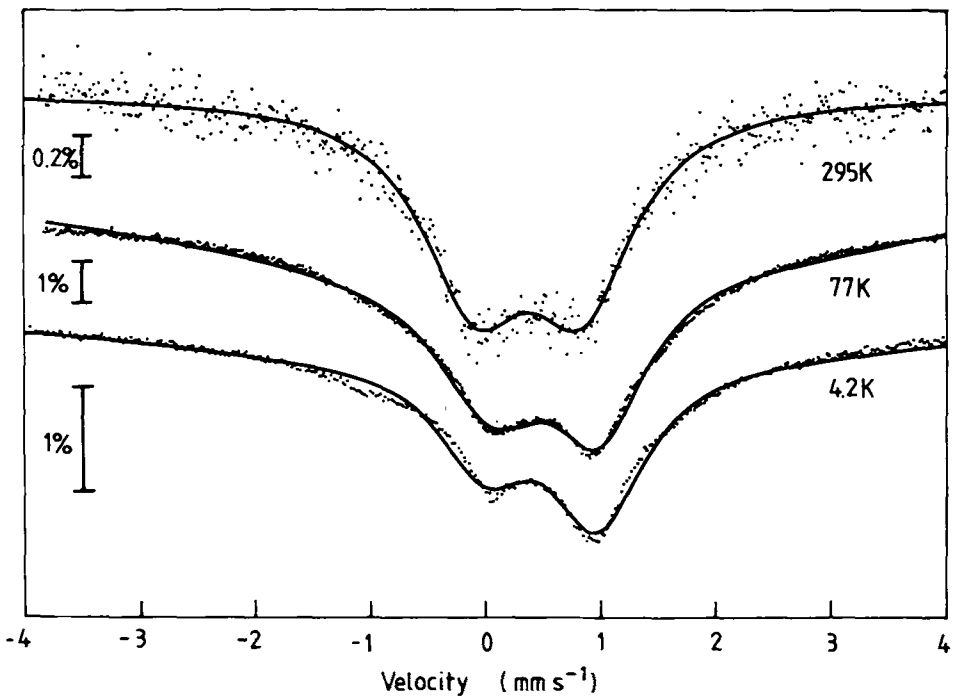

Figure 4. Mössbauer spectra of complex II in zero applied field at 295, 77 and 4·2 K. The solid lines represent fit 1 described in the text.

displaying appreciable ZFS. Thus μ_{Fe} remains constant at 5·9 B.M. above 20 K while below this it decreases rapidly to 5·3 B.M. at 4·2 K. Since the molecular symmetry of I, shown in figure 1 is clearly less than axial, the susceptibility data were fitted to the rhombic spin Hamiltonian

$$\mathcal{H} = g\beta\hat{H}.\hat{S} + D[\hat{S}_z^2 - 1/3S(S+1)] + E(\hat{S}_x^2 - \hat{S}_y^2].$$

Susceptibilities were calculated by means of a spatial averaging technique at the experimental magnetic field using the thermodynamic expression (Marathe and Mitra 1974; Vermaas and Groeneveld 1974; Mitra 1982). As has been noted previously, powder susceptibilities are only sensitive to the size of D and are insensitive to its sign and to the size of any rhombic splitting (Mitra 1982; Berry *et al* 1983). With these limitations in mind, and the knowledge that the Mössbauer spectral data suggest D to be negative, the present data could be reproduced very well with $D = -2{\cdot}4 \pm 0{\cdot}2$ cm^{-1}, $E = 0{\cdot}6 \pm 0{\cdot}2$ cm^{-1} and $g = 1{\cdot}98 \pm 0{\cdot}02$. It is interesting to note that there is no evidence for any weak exchange coupling via the H-bonded methanol network. This contrasts with the situation in [Fe(3-MeO-salen)(5-Ph-imd)(H_2O)]$^+$ in which H-bonding to the bonded water molecule occurs between pairs of cations (Kennedy *et al* 1985). The temperature dependent susceptibilities of the azide complex, II, are similar to those shown in figure 5, although the low temperature decrease in μ_{Fe} is somewhat less indicating a smaller ZFS. Best-fit parameters of $D = -1{\cdot}4 \pm 0{\cdot}2$ cm^{-1}, $E = 0{\cdot}4 \pm 0{\cdot}2$ cm^{-1} and $g = 2{\cdot}00 \pm 0{\cdot}01$ were obtained for II. There is no evidence from the μ_{Fe}/T data for

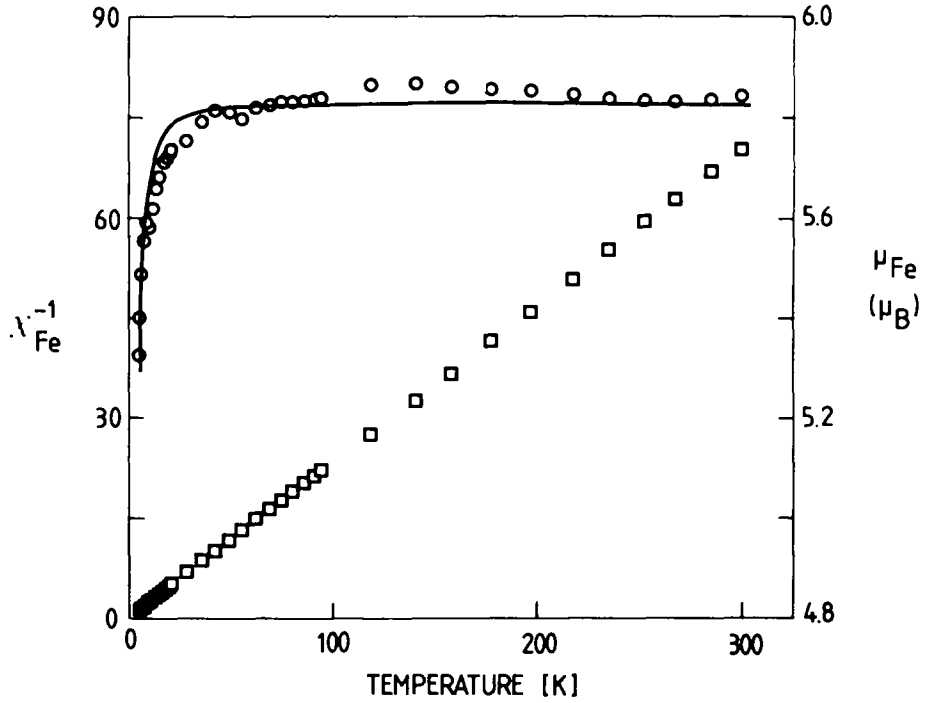

Figure 5. Magnetic moment (○) and reciprocal susceptibility (□) (per iron) versus temperature for complex I. The solid line represents the best fit of the data to the spin Hamiltonian in the text.

the presence of small quantities of an $S = 1/2$ contaminant, but this would be very hard to detect.

In principle ESR spectroscopy should provide a much more sensitive probe for rhombic splitting of the $^6A_1$ ground state than powder susceptibilities. A polycrystalline sample of II at 80 K showed a single broad resonance at $g \sim 4{\cdot}4$ (figure 6). The origin of such a line has been discussed elsewhere (Peisach and Blumberg 1971; Oosterhuis 1974) and in the present case can be thought to be due to appreciable rhombic splitting of the $^6A_1$ state with the ratio of E/D approaching 1/3 in reasonable agreement with the magnetic data. There was no evidence for any low-spin signals at $g \sim 2$, which might be expected in view of the Mössbauer spectra. However a low concentration of such species might be difficult to detect in the powder ESR spectrum. Under identical conditions, the ESR spectrum of a neat powdered sample of I surprisingly shows a single resonance at $g \sim 2{\cdot}1$. In frozen ethanol/chloroform glass, the spectrum of I does, however, show a strong line at

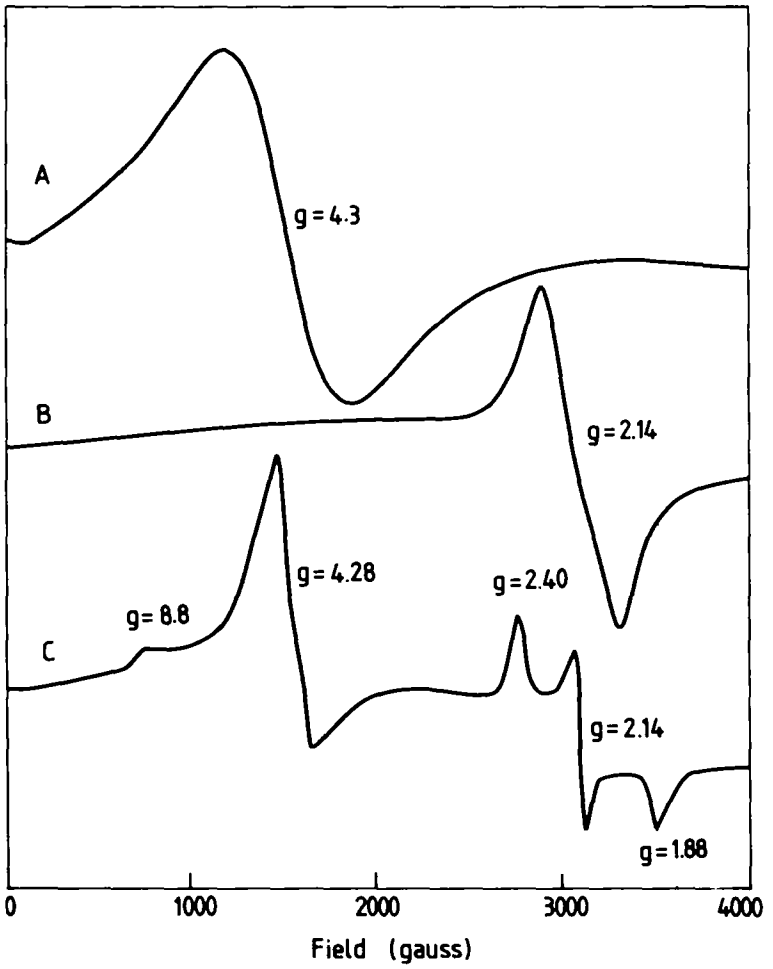

Figure 6. X-band ESR spectra at 80 K: (A) powder sample of II, (B) powder sample of I, (C) frozen glass ($EtOH/CHCl_3$) spectrum of I. The three lines at $g \sim 2$ are due to low-spin *bis*-imidazole species; see text.

g = 4·3 with somewhat weaker lines at g = 8·84, 2·40, 2·14 and 1·88. The lines at g = 8·84 and 4·3 can be attributed to high-spin Fe^{III} with $E/D \sim 1/3$ and are assigned to [(imd)Fe(salen)(NCS)]. The three lines near g = 2 in the frozen glass are due to a low-spin Fe^{III} complex which is formed in solution by the partial dissociation of the mono-adduct and subsequent formation of small amounts of the low-spin *bis*-imidazole adduct, i.e. $2[(imd)Fe(salen)(NCS)] \rightleftharpoons [(imd)_2Fe(salen)]NCS + Fe(salen)(NCS)$. Under similar conditions a sample of [Fe(salen)(NCS)] was ESR silent presumably because of exchange coupling between dimeric units as in $[Fe(salen)Cl]_2$. It is not clear why the neat solid spectrum of I should show a resonance at g = 2·1 and be different from that of II. Since the glass spectrum shows the g = 4·3 signal it seems likely that exchange effects rather than any fundamental difference in ligand-field splittings are causing the differences in the spectra. Somewhat related effects were observed in the high-spin complexes $[Fe(R\text{-}salen)(H_2O)L]BPh_4$, although the powder spectra in these cases tended to show lines at very low fields (Kennedy *et al* 1985). The sign of D was also reversed compared to I and II.

Finally, it is interesting to contemplate the possible reasons for a change in the sign of D in I and II compared to the $[Fe(R\text{-}salen)(H_2O)(5Ph\text{-}imd)]^+$ species (Kennedy *et al* 1985). Changes in the axial combination from $\{H_2O,5Ph\text{-}imd\}$ (D positive) to $\{NCS^-, imd\}$ (D negative) would appear to be the dominant cause. NCS^- generally has a marginally larger Dq value than H_2O and has more π-bonding capability than H_2O. The Fe–N(CS) distance is shorter than the Fe–O(H_2) distance while the Fe–N(imidazole) distances are the same. The in-plane Fe–O and Fe–N distances are slightly longer in I compared to $[Fe(3MeO\text{-}salen)(H_2O)(5Ph\text{-}imd)]BPh_4$. All these effects presumably combine to reverse the order of the low-lying quartet state sub-levels ($^4A_2$ or ^4E in D_{4h}), which is responsible for the size and sign of ZFS of the $^6A_1$ ground state. In order to probe further into the subtleties of these electronic features, experimental determinations of single-crystal magnetism, high-field magnetization and applied-field Mössbauer spectra would be required (Mitra 1982; Berry *et al* 1983; Kennedy and Murray 1985). Unfortunately the direct observation of excited ligand-field levels via visible spectroscopy is not possible in Fe^{III} Schiff-base systems because of overlying charge-transfer bands. From the theoretical point of view an angular overlap analysis of the σ- and π-bonding effects of the axial and in-plane ligands would be worthwhile in relation to the ground state ZFS, but this remains a formidable problem for d^5 high-spin configurations (Gerloch 1979).

Acknowledgements

This work was supported by grants from the Australian Research Grants Scheme (to KSM and MRS) and from the Monash University Special Research Grants (to KSM).

Supplementary material: Listings of fractional atomic coordinates and anisotropic thermal parameters, all bond lengths and angles, and the observed and calculated structure factor tables are available at the editorial office and with the authors.

References

Adams K M, Rasmussen P G, Scheidt W R and Hatano K 1979 *Inorg. Chem.* **18** 1892

Berry K J, Clark P E, Murray K S, Raston C and White A H 1983 *Inorg. Chem.* **22** 3928

Buckley A N, Herbert I R, Rumbold B D, Wilson G V H and Murray K S 1970 *J. Phys. Chem. Solids* **31** 1423

Buckley A N 1971 Ph.D. thesis, *Mössbauer effect investigation of some paramagnetic iron compounds* Monash University, Australia

Calligaris M, Nardin G and Randaccio L 1972 *Coord. Chem. Rev.* **7** 385

Clearfield A, Gopal R, Kline R J, Sipski M and Urban L O 1978 *J. Coord. Chem.* **7** 163

Collman J P, Sorell T N, Hodgson K G, Kulshrestha A K and Strouse C E 1978 *J. Am. Chem. Soc.* **99** 5180

Geiger D K, Chunplang V and Scheidt W R 1985 *Inorg. Chem.* **24** 4736

Gerloch M 1979 *Prog. Inorg. Chem.* **26** 1

Goldanskii V I, Makarov E F, Suzdalev I P and Vinogradov I A 1968 *Phys. Rev. Lett.* **20** 137

Gregson A K 1981 *Inorg. Chem.* **20** 81

Gulotti M, Casella L, Pasini A and Ugo R 1977 *J. Chem. Soc., Dalton Trans.* 339

Guss J M 1979 *SUSCAD, Program for Data Reduction for the CAD 4 diffractometer*, Univ. Sydney

Hill H A O, Skyte P D, Buchler J W, Leuken H, Tonn M, Gregson A K and Pellizer C J 1979 *J. Chem. Soc., Chem. Commun.* 151

Ibers J A and Hamilton W C 1974 *International tables for x-ray crystallography* (Birmingham: Kynoch Press) Vol. 4

Karyagin S V 1963 *Sov. Phys. Dokl. (Engl. Transl.)* **148** 110

Kennedy B J 1984 Ph.D. thesis, *Electronic structure of some transition metal paramagnets* Monash University, Australia

Kennedy B J, Brain G, Horn E, Murray K S and Snow M R 1985 *Inorg. Chem.* **24** 1647

Kennedy B J, Fallon G D, Gatehouse B M K C and Murray K S 1984 *Inorg. Chem.* **23** 580

Kennedy B J and Murray K S 1985 *Inorg. Chem.* **24** 1552

Kennedy B J, McGrath A C, Murray K S, Skelton B W and White A H 1987 *Inorg. Chem.* (in press)

Korszun Z R and Moffatt K 1981 *J. Mol. Biol.* **145** 815

La Mar G N and Walker F A 1972 *J. Am. Chem. Soc.* **94** 8607

Mackey D J, Evans S V and Martin R L 1976 *J. Chem. Soc., Dalton Trans.* 1515

Maeda Y, Ohshio H and Takashima Y 1982 *Chem. Lett.* 948

Marathe V R and Mitra S 1974 *Chem. Phys. Lett.* **27** 103

Mitchell A J, Murray K S, Newman P J and Clark P E 1977 *Aust. J. Chem.* **30** 2439

Mitra S 1982 *Iron porphyrins* (eds) H B Gray and A B P Lever (Reading: Addison-Wesley)

Nishida Y, Oshio S and Kida S 1975 *Chem. Lett. (Jpn.)* 79

Nishida Y, Oshio S and Kida S 1977 *Bull. Chem. Soc. Jpn.* **50** 119

Ohshio H, Maeda Y and Takashima Y 1983 *Inorg. Chem.* **22** 2684

Oosterhuis W T 1974 *Struct. Bonding (Berlin)* **20** 59

Peisach J and Blumberg W E 1971 *Probes of structure & function of macromolecules & enzymes* (eds) B Chance, T Yonetani and N S Mildvan (New York: Academic Press) p. 231

Satterlee J D, La Mar G N and Frye J S 1976 *J. Am. Chem. Soc.* **98** 7275

Scheidt W R, Cohen I A and Kastner M E 1979 *Biochemistry* **18** 3546

Scheidt W R, Geiger D K, Hayes R G and Lang G 1983a *J. Am. Chem. Soc.* **105** 2625, and references therein

Scheidt W R, Lee Y T, Geiger D K, Taylor K, and Hatano K 1982 *J. Am. Chem. Soc.* **104** 3367

Scheidt W R, Lee Y J, Luangdilov W, Haller K, Anzai K and Hatano K 1983b *Inorg. Chem.* **22** 1516

Scheidt W R and Reed C A 1981 *Chem. Rev.* **81** 543

Scoville A N and Reiff W M 1983 *Inorg. Chim. Acta* **70** 127

Sheldrick G M 1976 *SHELX, Program for crystal determination*, Univ. Cambridge, Cambridge, England

Vermaas A and Groeneveld W L 1974 *Chem. Phys. Lett.* **27** 583

Walker F A, Lo M W and Ree M T 1976 *J. Am. Chem. Soc.* **98** 5552